WNT/β-catenin pathway, the expression of *Dkk2* and *Wif1* was observed in eSZ cells expressing *EWS-FLI1* (Figure 5B and Figure 6B). *Dkk2* expression was comparable between parental eSZ and eGP cells, and *EWS-FLI1* introduction induced upregulation of *Dkk2* only in eSZ cells (Figure 5B and Figure 6B). In contrast, expression of *Dkk1*, which is antagonistic to DKK2, remained unaltered by *EWS-FLI1* introduction in eSZ cells. Higher *Wif1* expression was observed in eSZ cells but not in eGP cells, and the difference in expression between eSZ and eGP cells was preserved after *EWS-FLI1* introduction. The WNT/β-catenin pathway was not enriched when gene sets of nontransduced eSZ and eGP cells were tested (data not shown). In addition, gene sets for the EGF pathway and receptor protein kinase activity were enriched (Figure 6B and Supplemental Figure 8). *Prkcb1* is a gene downstream from EWS-FLI1 (39) and is inherently expressed at higher levels in eSZ cells than in eGP cells. Notably, its expression was increased to higher levels by introducing *EWS-FLI1* into eSZ cells. *Flt4* (also known as *VEGFR3*) and *Musk*, which are important in signaling of vascular and neuromuscular systems, were also identified as EWS-FLI1–responsive genes (Figure 6B and Supplemental Figure 8). Furthermore, IGF1R and IGF2R, which are involved in IGF1 signaling and are attractive targets in Ewing's sarcoma therapy (40, 41), were also identified by GSEA (Supplemental Figure 8).

Dkk2 is a member of the dickkopf family of proteins. As modulators of the WNT/β-catenin pathway, this family plays important roles in the development and homeostasis of bone and cartilage (42). A previous study showed that *DKK2* was downregulated upon *EWS-FLI1* knockdown in Ewing's sarcoma cells, while the opposite response was observed in *DKK1* (26). Although previous studies suggested that DKK1 and DKK2 might have functions independent of the canonical WNT/β-catenin pathway (43), possible roles of WNT activation in human Ewing's sarcoma were reported (44).

To confirm the involvement of the WNT/β-catenin pathway in tumorigenesis of Ewing's sarcoma, expression of β-catenin protein was evaluated. β-Catenin expression was increased by transient introduction of *EWS-FLI1* into eSZ cells (Supplemental Figure 9A). As described above, murine Ewing's sarcoma was serially transplantable into syngeneic mice and showed high potency of proliferation (Supplemental Figure 2C). In the invasive area of the secondary tumor, increased expression of β-catenin was frequently observed (Supplemental Figure 9B). RNA interference–mediated *EWS-FLI1* knockdown resulted in decreased transcriptional activities of β-catenin (Supplemental Figure 9C). Collectively, these data indicate strong association between the upregulation of WNT/β-catenin signaling and cell growth of Ewing's sarcoma.

Inhibition of tumor growth by suppression of critical signals. The result indicates that EWS-FLI1 and its downstream signals are effective targets for therapy. Indeed, gene knockdown experiments showed that tumor cell proliferation was significantly inhibited by siRNA treatments specific for *Fli1*, *Dkk2*, *Catnb*, *Prkcb1*, *Ezh2*, or *Igf1* (Figure 6C). Knockdown of the same genes in the human Ewing's sarcoma cells showed similar suppression of cell proliferation (Supplemental Figure 10). Moreover, suppression of the EGF/RAS/MAPK pathway by a MEK1 inhibitor (U0126) showed inhibition of tumor growth in vitro in a dose-responsive manner (Figure 6D). These results demonstrated the importance of the signaling pathways activated by EWS-FLI1 in the progression of Ewing's sarcoma and its potential as a novel target for clinical treatment.

Use of the mouse model to test therapy targeted against Ewing's sarcoma. Animal models of human cancer provide platforms for evaluation of novel therapies. Ideally, the phenotypes and developmental mechanisms of the human and model systems should be similar. In this context, specific inhibitors of the WNT/β-catenin pathway, EZH2 and poly (ADP-ribose) polymerase 1 (PARP1), were tested using the current model both in vitro and in vivo. The β-catenin inhibitors, iCRT14 and PNU74654, showed marked growth suppression of both mouse and human Ewing's sarcoma, and an EZH2 inhibitor DZNeP showed modest but substantial growth suppression (Figure 7A and Table 3). Moreover, olaparib, a PARP1 inhibitor reported to exhibit Ewing's sarcoma–specific growth inhibition (45), also inhibited both mouse and human Ewing's sarcomas (Figure 7A and Table 3). Cell cycle analyses showed that iCRT14 and DZNeP induced cell cycle arrest, as indicated by increased G_1 populations and decreased G_2/M populations (Figure 7B). PNU74654 and olaparib also increased a sub-G_1 population, indicating apoptosis induction (Figure 7B). These reagents also suppressed in vivo growth of Ewing's sarcoma, with the greatest effect observed with iCRT14, followed by olaparib, DZNeP, and PNU74654 (Figure 7C). Thus, the current model provides an effective tool to explore and evaluate novel therapeutic drugs both in vitro and in vivo.

Discussion

Here, we demonstrate efficient and specific induction of a mouse equivalent of human Ewing's sarcoma. We showed that the origin of the tumor is closely related to embryonic osteochondrogenic progenitor cells. Selection of a PTHLH-expressing cellular fraction in eSZ enabled us to obtain substantially higher efficiency and greater specificity and consistency of tumor formation than previously reported investigations using bone marrow–derived mesenchymal stem/progenitor cells (9, 10). In addition, *EWS-FLI1* expression induced apoptosis and growth arrest in several cell types, including embryonic fibroblasts (46, 47). These data indicate that induction of Ewing's sarcoma by *EWS-ETS* fusion genes is much more effective for progenitor cells of a certain cell lineage, including the osteochondrogenic axis, especially in developing bone. A previous study indicated that *EWS-FLI1* induces cancer stem cell properties in pediatric MSCs but not in adult MSCs (48). The plasticity for cellular differentiation in embryonic and pediatric precursor cells might be important for Ewing's sarcoma development in younger patients. Moreover, EWS-ETS might induce the development of small round cells and neuroectoderm-like phenotypes.

Ewing's sarcoma is a rather rare neoplasm that affects children and adolescents with an incidence of 2.1 cases per million children (49). The low incidence of disease is also observed in other translocation-related sarcomas affecting young people, such as alveolar rhabdomyosarcoma, clear cell sarcoma, synovial sarcoma, or myxoid liposarcoma (50). This is in contrast to acute myeloid leukemia (AML), which is also characterized by gene fusion. It is likely that the difference in frequencies between sarcomas and AMLs is due to the rarity of progenitor cell populations in which chromatin conditions necessary for the oncogenic action of EWS-ETS are present. Such a narrow window of target cell emergence reflects the difficulty of inducing tumor in vivo models.

Once the EWS-FLI1 fusion occurs in an eSZ cell during the perinatal period or even in utero, the cell survives with acquired growth advantages. After a decade of incubation that allows additional genetic/epigenetic events in the mutated eSZ cell, Ewing's sarcoma eventually emerges in the bone as a highly aggressive tumor in human child-

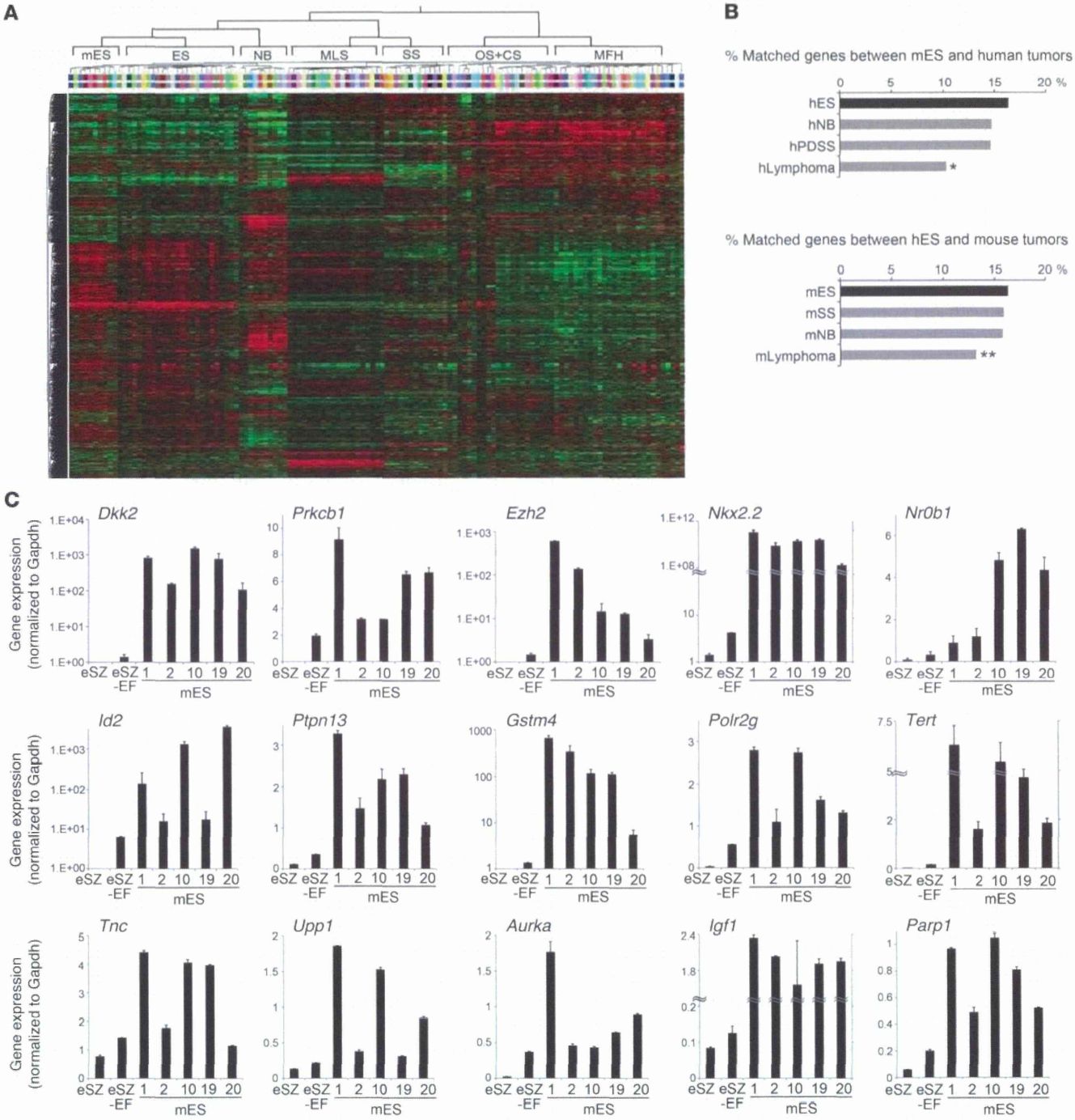

Figure 4

Clustering analysis of murine and human sarcomas. (**A**) Supervised clustering of gene expression profiles of 10 samples of murine Ewing's sarcomas (mES), 32 cases of human Ewing's sarcomas (ES), 21 malignant fibrous histiocytomas (MFH), 20 myxoid liposarcomas (MLS), 16 synovial sarcomas (SS), 11 osteosarcomas (OS), 10 neuroblastomas (NB) and 7 chondrosarcomas (CS). (**B**) Gene expression profiles of mouse and human Ewing's sarcoma (hES) were compared with those of other small round cell tumors of the other species. The frequencies of matched genes in 2,000 gene sets are indicated. Expression profiles of 6 human poorly differentiated synovial sarcoma (hPDSS) cases, 14 cases of human malignant lymphoma, 5 samples of murine synovial sarcoma, 7 murine neuroblastomas, and 6 murine malignant lymphoma were examined. (**C**) Quantitative RT-PCR for upregulated genes common between eSZ cells with *EWS-FLI1* (EF) and murine Ewing's sarcomas. The numbers listed above "mES" denote tumor IDs. The mean ± SEM of 3 independent experiments are shown. $^{*}P < 0.001$ vs. hES; $^{**}P < 0.01$ vs. mES.

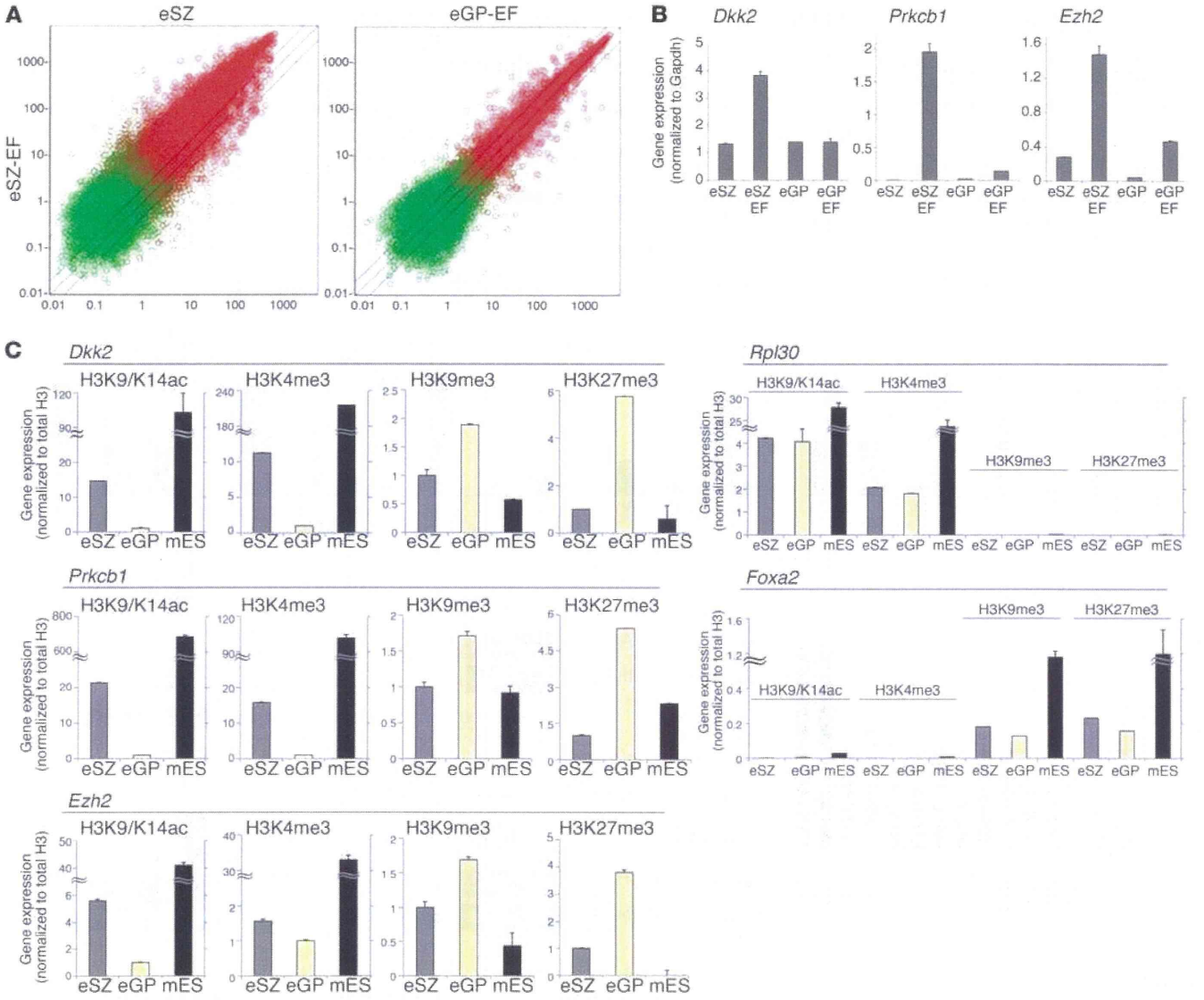

Figure 5

Differences in gene expression between eSZ and eGP cells. (**A**) Comparison of gene expression profiles between eSZ/*EWS-FLI1* and eSZ and eSZ/*EWS-FLI1* and eGP/*EWS-FLI1* 48 hours after introduction. Scatter plots of eSZ with (vertical axis) or without *EWS-FLI1* (horizontal axis) and eSZ with *EWS-FLI1* (vertical axis) or eGP with *EWS-FLI1* (horizontal axis) are shown. Red dots indicate probes of present call, and green dots indicate those of absent call. The threshold lines above and below the diagonal indicate $y = 2x$ (2-fold increase) and $y = 0.5x$ (2-fold decrease), respectively. (**B**) Expression patterns of *Dkk2*, *Prkcb1*, and *Ezh2* were validated by quantitative RT-PCR. The mean ± SEM of 3 independent experiments are shown. (**C**) ChIP-PCR for histone modification at *Dkk2*, *Prkcb1*, and *Ezh2* promoter regions in eSZ, eGP, and murine Ewing's sarcomas. *Rpl30* and *Foxa2* were used as controls for active and repressive histone marks, respectively. The mean ± SEM of 3 independent experiments are shown.

hood. This scenario explains why the location of Ewing's sarcoma is different from that of osteosarcoma, which is frequently observed in the metaphysis of long bones. There is a variant of human Ewing's sarcoma that develops in the soft tissue and is also characterized by the invariable *EWS-ETS* fusion. As the origin of Ewing's sarcoma in the soft tissue remains to be clarified, the relatively late onset of the tumor suggests that dysregulation of the differentiation program in the mesenchymal system might play some role in its tumorigenesis.

Upregulation of the WNT/β-catenin pathway is a direct effect of EWS-ETS expression in preneoplastic and sarcoma cells, at least in part. However, rather mild β-catenin induction by EWS-FLI1 in the eSZ (Supplemental Figure 9A) suggests that additional genetic events might be required for constitutive activation of the pathway. Pathways involving receptor tyrosine kinases are also important in Ewing's sarcoma (40, 51), as was indicated in our model. Indeed, potential clinical benefits from the use of pazopanib, a multikinase inhibitor, for the treatment of childhood sarcoma, including Ewing's sarcoma, have been reported recently (52).

Tumor formation in our mouse model of Ewing's sarcoma was *EWS-ETS* dependent, as was clearly exhibited by *Cre/loxP*-mediated knockout experiments. This finding suggests that therapeutic

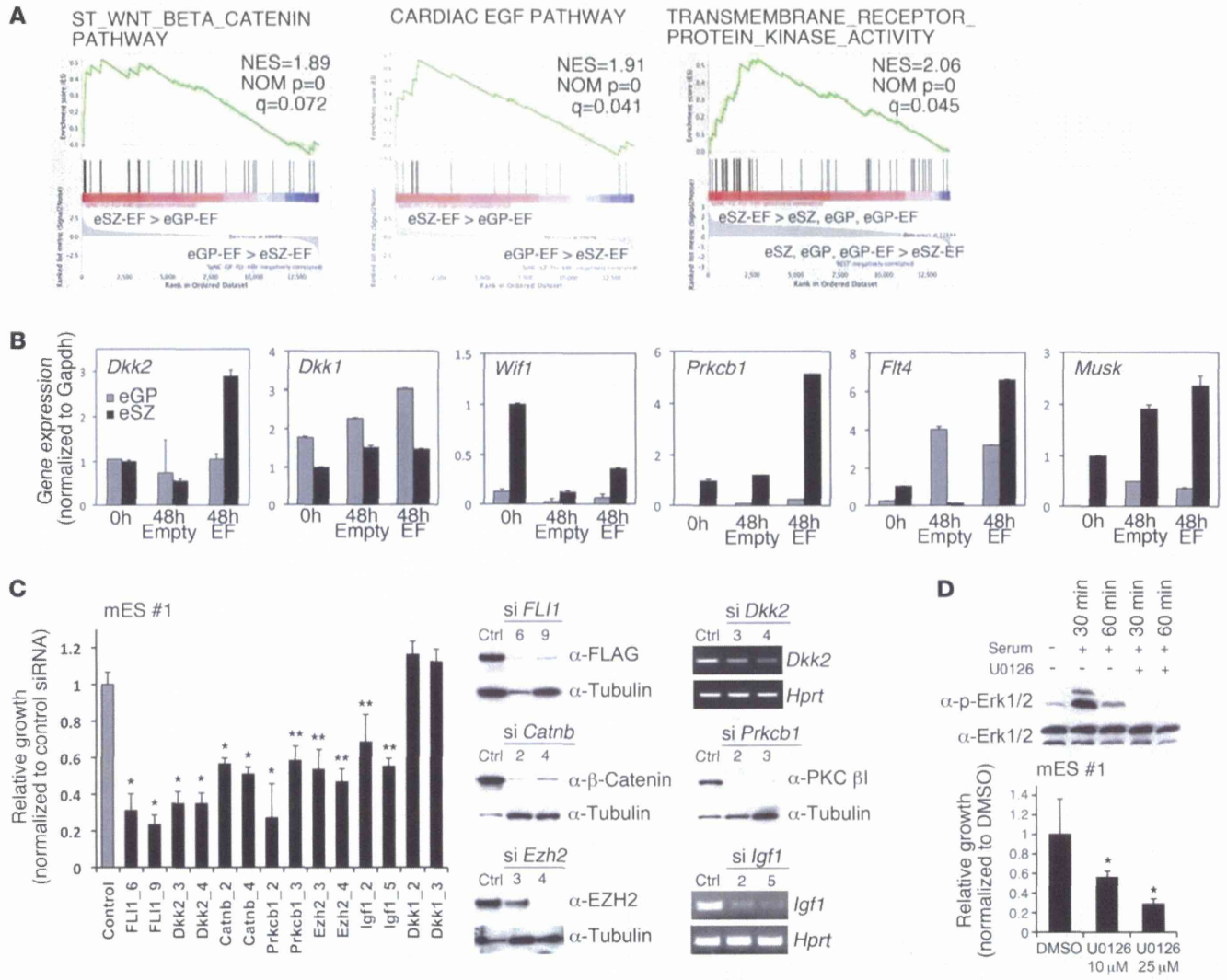

Figure 6

Modulation of gene expression and growth suppression of tumor cells by gene silencing. (**A**) GSEA of eSZ and eGP cells with *EWS-FLI1* (left and central panels) and between eSZ/*EWS-FLI1* and eGP, eSZ, and eGP/*EWS-FLI1* (right) resulted in enrichment of the WNT/β-catenin pathway, the EGF pathway, and receptor tyrosine kinase activities. (**B**) Real-time quantitative RT-PCR for *Dkk2*, *Dkk1*, *Wif1*, *Prkcb1*, *Flt4*, and *Musk* in eSZ or eGP cells with/without *EWS-FLI1* at 0 or 48 hours after introduction. The mean ± SEM of 3 independent experiments are shown. (**C**) Inhibition of cell proliferation by knockdown of *EWS-FLI1* and genes of the pathways specified in **A**. Relative growth of tumor cells 48 hours after siRNA treatment was calculated by comparing each cell number to cells treated with control siRNA. The symbols of siRNA used are indicated. *Dkk1* was tested as a negative control. Gene knockdown was confirmed by immunoblotting (*Fli1*, *Catnb*, *Ezh2*, and *Prkcb1*) or RT-PCR (*Dkk2* and *Igf1*). The experiment was repeated 3 times, and representative results are shown. (**D**) Effect of MAPK pathway inhibition on tumor growth. Erk phosphorylation was inhibited by a MEK1/2 inhibitor U0126 (10 μM) (top), and tumor proliferation was inhibited in a dose-dependent manner 48 hours after treatment (bottom). The mean ± SEM of 3 independent experiments are shown. $^*P < 0.01$; $^{**}P < 0.02$.

approaches should pursue the direct targeting of EWS-ETS as well as related pathways. Gene knockdown experiments and screening of inhibitory drugs in our model should prove valuable. Unlike the xenograft model of human cancer cells, the present mouse model excludes the unexpected bias caused by rather low penetrance of transplantation, an altered relationship between tumor cells and the microenvironment, and defects in certain signaling pathways due to differences in species-dependent binding affinities between ligands and receptors. Thus, our platform will allow us to explore and evaluate novel targeted therapies in combination with tests using human Ewing's sarcoma cell lines.

In summary, purification of the targets of primary oncogenic stimuli permitted us to establish a mouse model that closely recapitulates important characteristics of human Ewing's sarcoma. Taken together, the efficiency of tumor induction and the gene expression analyses of both the very limited cell population obtained by laser microdissection and the early neoplastic lesion strongly suggest that the cell of origin of Ewing's sarcoma is enriched in the eSZ cells. The present ex vivo method could be useful for generating other important animal models for human cancers, particularly when conventional transgenic models are driven by a gene expression-based method that is not always successful at

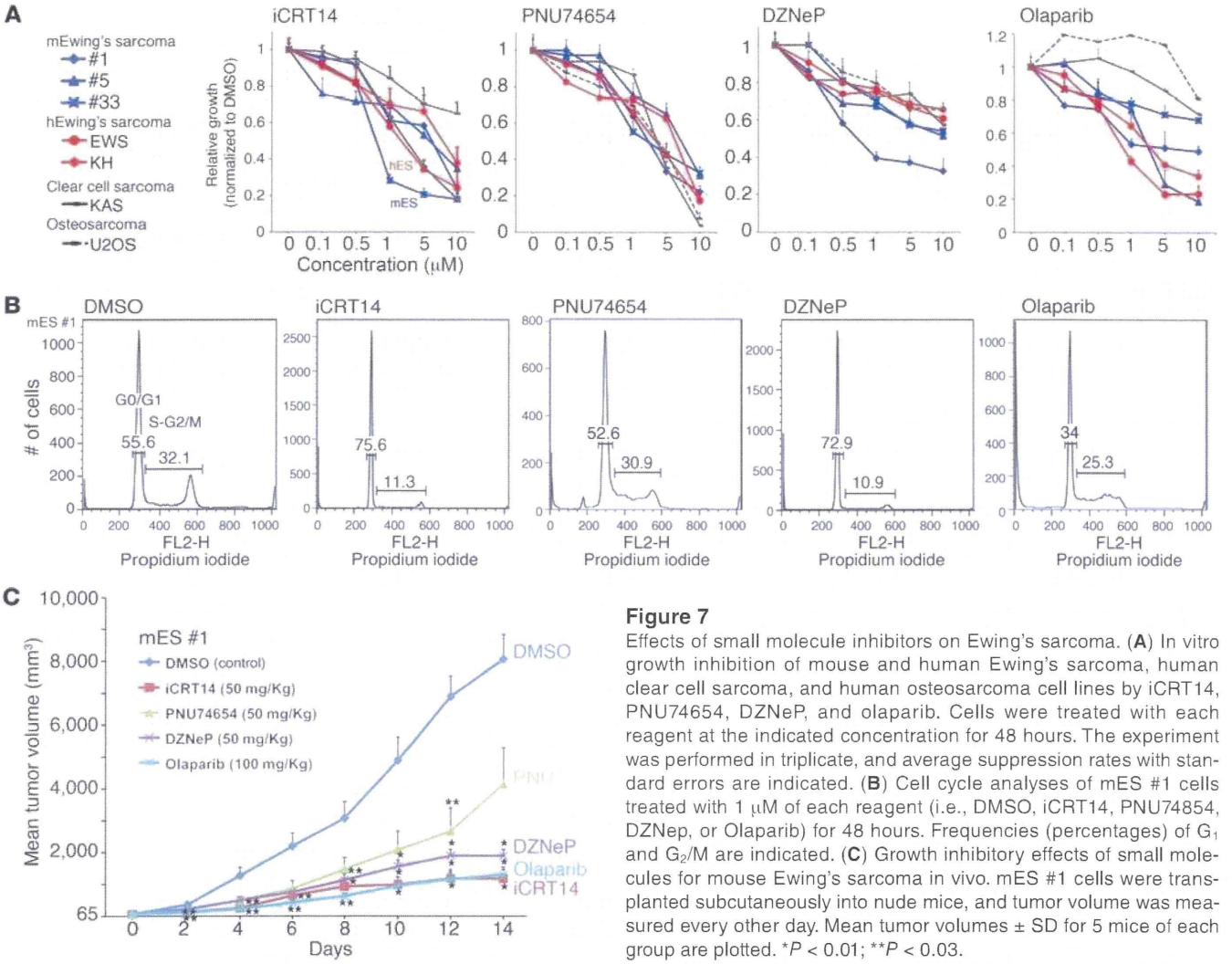

Figure 7

Effects of small molecule inhibitors on Ewing's sarcoma. (**A**) In vitro growth inhibition of mouse and human Ewing's sarcoma, human clear cell sarcoma, and human osteosarcoma cell lines by iCRT14, PNU74654, DZNeP, and olaparib. Cells were treated with each reagent at the indicated concentration for 48 hours. The experiment was performed in triplicate, and average suppression rates with standard errors are indicated. (**B**) Cell cycle analyses of mES #1 cells treated with 1 μM of each reagent (i.e., DMSO, iCRT14, PNU74854, DZNep, or Olaparib) for 48 hours. Frequencies (percentages) of G_1 and G_2/M are indicated. (**C**) Growth inhibitory effects of small molecules for mouse Ewing's sarcoma in vivo. mES #1 cells were transplanted subcutaneously into nude mice, and tumor volume was measured every other day. Mean tumor volumes ± SD for 5 mice of each group are plotted. $^*P < 0.01$; $^{**}P < 0.03$.

targeting exact cell types. The plasticity of precursor cells as well as their oncogenic potency due to chimeric transcription factors can be evaluated by the present approach and constitutes a useful tool for clarifying oncogenic mechanisms of childhood cancer.

Methods

Purification of eSZ cells. Femoral and humeral bones of BALB/c mouse embryos were removed aseptically on 18.5 dpc, and they were microdissected into eSZ, eGP, and eSyR under a stereomicroscope (Zeiss Stemi 2000-C, Carl Zeiss MicroImaging). Embryonic mesenchymal cells of the head or trunk were also prepared from the same embryos during each experiment. Each region was minced and gently digested with 2 mg/ml collagenase (Wako Pure Chemical) at 37°C for 2 hours. They were cultured in growth medium composed of Iscove's Modified Dulbecco's Medium (Invitrogen) supplemented with 15% fetal bovine serum and subjected immediately to retroviral infection. Fractionation of $PTHLH^+$ and $PTHLH^-$ eSZ populations was achieved using a rabbit anti-PTHLH (Abcam) and a CELLection Biotin Binder Kit (Dynal) according to the manufacturer's protocol. The frequency of the $PTHLH^+$ cells reached 8.3% of total eSZ cells (12-fold enrichment).

Retroviral infection and transplantation. N-terminal FLAG-tagged *EWS-FLI1* and *EWS-ERG* were introduced into the pMYs-IRES-GFP or pMYs-IRES-Neo vectors. The full-length *EWS-FLI1* cDNA was a gift from Susanne Baker (St. Jude Children's Research Hospital, Memphis, Tennessee, USA), and *EWS-ERG* was cloned from a human Ewing's sarcoma case. Retroviral infections of eSZ, eGP, or shaft cells were performed as described previously (53). Infection efficiency was examined using a FACSCalibur flow cytometer (Becton Dickinson). After 48 hours of spin infection, the cells were mixed with growth factor–reduced Matrigel (Becton Dickinson) and were transplanted subcutaneously to BALB/c nude mice. The mice were observed daily to check for tumor formation and general condition. Tumors were resected and subjected to further examination when subcutaneous masses reached 15 mm in diameter. Some tumors (1×10^6 cells) were serially transplanted subcutaneously or injected into the tail veins (1×10^6 cells) of nude mice to confirm tumorigenicity and metastatic activities.

Histopathology and immunohistochemistry. Formaldehyde- or paraformaldehyde-fixed tumor tissues were embedded in paraffin, and sections were stained with hematoxylin and eosin using standard techniques. Bromodeoxyuridine (BrdU) labeling was achieved by intraperitoneal injection of 1 mg/ml BrdU 30 minutes before sacrifice. eSZ cells were cultured on chamber slides and were fixed with 100% methanol. EWS-FLI1 and EWS-ERG antigens were detected using a polyclonal rabbit anti-FLAG antibody (Sigma-Aldrich) in conjunction with the VECTOR M.O.M. Immunodetection Kit (Vector Laboratories) or FITC-conjugated anti-rabbit immunoglobulin. The following primary antibodies were used: anti-BrdU (Molecular

Table 3
IC_{50} values of inhibitors

	Inhibitors			
Tumor cells	iCRT14 (μM)	PNU74654 (μM)	DZNeP (μM)	Olaparib (μM)
mES #1	5.90	2.08	0.68	7.07
mES #5	5.61	6.79	10.30	2.36
mES #33	0.76	1.96	10.95	17.50
hES_EWS	1.71	2.98	13.46	0.86
hES_KH	7.41	6.05	15.87	2.70
hCCS_KAS	2.16	3.16	16.58	28.85
hOS_U2OS	14.79	3.42	19.33	40.42

Probes), anti-mouse CD99 (a gift of Dietmar Vestweber, Max Planck Institute for Molecular Biomedicine, Muenster, Germany), anti-COL2A (Millipore), anti-S100 (Dako), anti-COL10 (SLS), anti-CD57 (Sigma-Aldrich), anti-NGFR (Millipore), anti–β-catenin (Becton Dickinson), anti-nestin (Chemicon), and anti-myosin (Nichirei). Immunofluorescent images were photographed with a Zeiss LSM 710 laser scanning microscope with a ×40 objective (Zeiss) and LSM Software ZEN 2009 (Zeiss).

Western blotting. Western blot analysis was performed using lysates of whole tumor tissues as described previously (54).

RT-PCR and real-time quantitative RT-PCR. Total RNA extraction, reverse transcription, and RNA quantification were performed according to methods described previously (54). Conventional RT-PCR and real-time quantitative RT-PCR were performed by using a Gene Amp 9700 thermal cycler (Applied Biosystems) and a 7500 Fast Real-Time PCR System (Applied Biosystems), respectively. The sequences of the oligonucleotide primers are shown in Supplemental Excel File 6.

Luciferase assay. A 1,340-bp genomic DNA fragment upstream from the murine *Gdf5* exon 1 was amplified by PCR using the following primers: forward (5′-TTCTATAATCCTACTCTGTAG-3′) and reverse (5′-CTGAAAATAACTCGTTCTTG-3′). The fragment was inserted into the pGL4.10 vector (Promega) and transfected into eSZ, eGP, eSyR, or trunk cells using Lipofectamine 2000 (Invitrogen). Luciferase assays were performed as described previously (54).

In vitro differentiation assay. Cells were plated at 2×10^5 cells per well in 6-well plates and cultured in growth medium. Adipogenic, chondrogenic, osteogenic, myogenic, and neurogenic differentiation assays were conducted according to the methods previously described (55–57).

Microarray analysis. GeneChip analysis was conducted to determine gene expression profiles. A per cell normalization method was applied to eSZ and eGP samples (58). Briefly, cellular lysates were prepared with RLT buffer (QIAGEN). After RNA cocktails were added to the cell lysates according to the amount of DNA, total RNA was extracted using the RNeasy Mini Kit (QIAGEN). The murine Genome 430 2.0 Array (Affymetrix) was hybridized with aRNA probes generated from eSZ and eGP cells and murine Ewing's sarcoma tissue. After staining with streptavidin-phycoerythrin conjugates, arrays were scanned using an Affymetrix GeneChip Scanner 3000 and analyzed using Affymetrix GeneChip Command Console Software (Affymetrix) and GeneSpring GX 11.0.2 (Agilent Technologies) as described previously (59). The expression data for eSZ and eGP cells were converted to mRNA copy numbers per cell by the Percellome method, quality controlled, and analyzed using Percellome software (58). GSEA was performed using GSEA-P 2.0 software (60).

Data comparisons and clustering between murine and human microarray data sets. The microarray data from 10 murine Ewing's sarcoma samples were compared with human microarray data sets. Data from the ONCOMINE database (https://www.oncomine.org/) were accessed in June 2011. Five microarray studies containing 117 tumor samples that were analyzed using Human Genome U133A Array (Affymetrix) were queried for gene expression. CEL files from E-MEXP-353 (61), E-MEXP-1142 (62), GSE6481 (63), GSE7529 (64), GSE21122 (65), GSE6461 (66), GSE42548 (67), GSE23972 (68), GSE20196 (69), and GSE10172 (70) were downloaded. The probe sets of the human U133A array were translated into 23,860 murine 430 2.0 arrays by the translation function of GeneSpring using Entrez Gene ID to make a novel common platform. Hierarchical clustering was achieved using log-transformed data and the following procedure. For the initial statistical analysis, 13,026 genes that showed a "present" or "marginal" call in at least 24 of a total of 32 human Ewing's sarcoma samples were selected. Then, 12,340 probes were selected by 1-way ANOVA ($P < 0.05$) analysis. Finally, 1,819 probes that showed >2-fold differences of expression in at least 3 tumor types were selected. With these 1,819 probes, hierarchical clustering was performed using the average linkage method and the Pearson's centered measurements. In addition, a probe set consisting of the 2,000 sequences that were the most altered in expression in human and mouse round cell tumors (Ewing's sarcoma, neuroblastoma, poorly differentiated synovial sarcoma, and malignant lymphoma) was used to distinguish each tumor from the other 3 using a fold-change analysis. Then, the frequencies of these 2,000 probes were compared between mouse Ewing's sarcoma and 4 human tumor types and between human Ewing's sarcoma and 4 mouse tumor types to find the closest tumor type using similar entities from GeneSpring.

ChIP. A total of 5×10^6 cells per immunoprecipitation were cross-linked with 10% formaldehyde for 10 minutes at room temperature. Histone immunoprecipitation was performed with anti-histone antibodies targeted against H3K9/K14Ac, H3K4/me3, H3K27/me3, total H3 (Cell Signaling Technologies), or H3K9/me3 (Millipore) preconjugated to protein G magnetic beads. Immunoprecipitated DNA was amplified with primers specific for each region. Sequences are shown in Supplemental Excel File 6.

Cre/loxP-mediated gene silencing. eSZ cells were transduced with a floxed *EWS-FLI1* retrovirus, and Ewing's sarcoma cells were obtained from a subcutaneous tumor developed in a nude mouse. Tumor cells were transduced with pMSCV-Cre-puro retrovirus in vitro. Senescence-associated β-galactosidase expression was detected using a Senescence Detection Kit (Biovision) 4 days after transduction of the retrovirus.

siRNA interference studies. For knockdown of *FLI1*, *Dkk2*, *Catnb*, *Prkcb1*, *Ezh2*, *Igf1*, *Dkk1*, and *Erg*, siRNAs were purchased from QIAGEN. The list of siRNAs is shown in Supplemental Excel File 7. siRNAs were introduced into mouse Ewing's sarcoma cells according to the manufacturer's protocol. Knockdown efficiencies were confirmed by Western blotting using anti-FLAG (Sigma-Aldrich), anti-ERG and anti–PKC β1 (Santa Cruz Biotechnology), anti–β-catenin (Becton Dickinson), and anti-EZH2 (Cell Signaling Technologies) or RT-PCR.

Pharmacological experiments with specific inhibitors. Mouse Ewing's sarcoma cells were treated with MEK1 inhibitor U0126 (Cell Signaling Technologies) in vitro. Both mouse and human Ewing's sarcoma cell lines were treated with WNT/β-catenin inhibitors, iCRT14 and PNU74654 (Tocris Bioscience); an EZH2 inhibitor, DZNeP (Cayman Chemical); or a PARP1 inhibitor, olaparib (Selleckchem), both in vitro and in vivo. Inhibition of ERG phosphorylation was examined by Western blotting using anti–P-ERK1/2 and anti-ERK1/2 (Cell Signaling

Technologies). For in vivo experiments, 1×10^6 tumor cells were transplanted subcutaneously into nude mice, and the mice were treated with specific inhibitors when the tumor diameter reached 5 mm. All the inhibitors were dissolved in 0.2% DMSO, and they were administered by intraperitoneal injection 3 times per week.

Cell cycle assay. Single-cell suspensions were permeabilized with 0.1% Triton X-100 in PBS, and 50 mg/ml propidium iodide and 1 mg/ml RNAse A were added. The cell suspensions were then analyzed by using a FACSCalibur flow cytometer and ModFit software (Becton Dickinson).

Cloning retroviral integration sites. Retroviral integration sites of individual mouse Ewing's sarcoma were isolated by inverse PCR, sequenced, and mapped as described previously (71).

Accession numbers. The microarray data sets are accessible through the NCBI Gene Expression Omnibus (GEO) database (http://www.ncbi.nlm.nih.gov/geo), with accession numbers GSE32615 and GSE32618.

Statistics. Continuous distributions were compared with 2-tailed Student's *t* test. Survival analysis was performed using the Kaplan-Meier life table method, and survival between groups was compared with the log-rank test. The 2-proportion z test was used to evaluate the significance of differences in the matched probe sets between 2 tumor types. All *P* values were 2 sided, and a *P* value of less than 0.05 was considered significant.

Study approval. Animals were handled in accordance with the guidelines of the animal care committee at the Japanese Foundation for Cancer Research, which gave ethical approval for these studies.

Acknowledgments

We thank W. Kurihara and T. Koui for helping with the microarray analyses; S.J. Baker (St Jude Children's Research Hospital, Memphis, Tennessee, USA) for EWS-FLI1 cDNA; and D. Vestweber (Max Planck Institute for Molecular Biomedicine, Muenster, Germany) for anti-mouse CD99. The research was funded by Grant-in-Aid for Scientific Research on Priority Areas Cancer 17013086 from Ministry of Education, Culture, Sports, Science and Technology and Grant-in-Aid for Young Scientists 23791672 from Japan Society for the Promotion of Science.

Received for publication July 29, 2013, and accepted in revised form April 10, 2014.

Address correspondence to: Takuro Nakamura, 3-8-31 Ariake, Koto-ku, Tokyo 135-8550, Japan. Phone: 81.3.3570.0462; Fax: 81.3.3570.0463; E-mail: takuro-ind@umin.net.

1. Bernstein M, et al. Ewing's sarcoma family of tumors: current management. *Oncologist.* 2006;11(5):503–519.
2. Ewing J. Diffuse endothelioma of bone. *Proc New York Pathol Soc.* 1921;21:17–24.
3. Hu-Lieskovan S, Zhang J, Wu L, Shimada H, Schofield DE, Triche TJ. EWS-FLI1 fusion protein up-regulates critical genes in neural crest development and is responsible for the observed phenotype of Ewing's family of tumors. *Cancer Res.* 2005;65(11):4633–4644.
4. Tirode F, Laud-Duval K, Prieur A, Delorme B, Cahrbord P, Delattre O. Mesenchymal stem cell features of Ewing tumors. *Cancer Cell.* 2007;11(5):421–429.
5. Delattre O, et al. Gene fusion with an ETS DNA-binding domain caused by chromosome translocation in human tumours. *Nature.* 1992;359(6391):162–165.
6. Zucman J, et al. Combinatorial generation of variable fusion proteins in the Ewing family of tumours. *EMBO J.* 1993;12(12):4481–4487.
7. Sorensen PH, Lessnick SL, Lopez-Terrada D, Liu XF, Triche TJ, Denny CT. A second Ewing's sarcoma translocation, t(21;22), fuses the EWS gene to another ETS-family transcription factor, ERG. *Nat Genet.* 1994;6(2):146–151.
8. Ordonez JL, Osuna D, Herrero D, de Alava E, Madoz-Gurpide J. Advances in Ewing's sarcoma research: where are we now and what lies ahead? *Cancer Res.* 2009;69(18):7140–7150.
9. Riggi N, et al. Development of Ewing's sarcoma from primary bone marrow-derived mesenchymal progenitor cells. *Cancer Res.* 2005;65(24):11459–11468.
10. Castillero-Trejo Y, Eliazer S, Xiang L, Richardson JA, Ilaria RL Jr. Expression of the EWS/FLI-1 oncogene in murine primary bone-derived cells results in EWS/FLI-1-dependent, Ewing sarcoma-like tumors. *Cancer Res.* 2005;65(19):8698–8705.
11. Arndt CAS, Crist WM. Common musculoskeletal tumors of childhood and adolescence. *N Engl J Med.* 1999;341(5):342–352.
12. Iwamoto M, et al. 2007. Transcription factor ERG and joint and articular cartilage formation during mouse limb and spine skeletogenesis. *Dev Biol.* 2007;305(1):40–51.
13. Koyama E, et al. A distinct cohort of progenitor cells participates in synovial joint and articular cartilage formation during mouse limb skeletogenesis. *Dev Biol.* 2008;316(1):62–73.
14. Mundy C, et al. Synovial joint formation requires local Ext1 expression and heparin sulfate production in developing mouse embryo limbs and spine. *Dev Biol.* 2011;351(1):70–81.
15. Ambros IM, Ambros PF, Strehl S, Kovar H, Gadner H, Salzer-Kuntschik M. MIC2 is a specific marker for Ewing's sarcoma and peripheral primitive neuroectodermal tumors. Evidence for a common histogenesis of Ewing's sarcoma and peripheral primitive neuroectodermal tumors from MIC2 expression and specific chromosome aberration. *Cancer.* 1991;67(7):1886–1893.
16. Bixel G, Kloep S, Butz S, Petri B, Engelhardt B, Vestweber D. Mouse CD99 participates in T-cell recruitment into inflamed skin. *Blood.* 2004;104(10):3205–3213.
17. Vortkamp A, Lee K, Lanske B, Segre GV, Kronenberg HM, Tabin CJ. Regulation of rate of cartilage differentiation by Indian Hedgehog and PTH-related protein. *Science.* 1996;273(5275):613–622.
18. Sohaskey ML, Yu J, Diaz MA, Plaas AH, Harland RM. JAWS coordinates chondrogenesis and synovial joint positioning. *Development.* 2008;135(13):2215–2220.
19. Vijayaraj P, et al. Erg is a crucial regulator of endocardial-mesenchymal transformation during cardiac valve morphogenesis. *Development.* 2012;139(21):3973–3985.
20. Storm EE, Kingsley DM. GDF5 coordinates bone and joint formation during digit development. *Dev Biol.* 1999;209(1):11–27.
21. St-Jacques B, Hammerschmidt M, McMahon AP. Indian hedgehog signaling regulates proliferation and differentiation of chondrocytes and is essential for bone formation. *Genes Dev.* 1999;13(16):2072–2086.
22. Mak KK, Kronenberg HM, Chuang PT, Mackem S, Yang Y. Indian hedgehog signals independently of PTHrP to promote chondrocyte hypertrophy. *Development.* 2008;135(11):1947–1956.
23. Toomey EC, Schiffman JD, Lessnick SL. Recent advances in the molecular pathogenesis of Ewing's sarcoma. *Oncogene.* 2010;29(32):4504–4516.
24. James CG, Stanton LA, Agoston H, Ulici V, Underhill TM, Beier F. Genome-wide analyses of gene expression during mouse endochondral ossification. *PLoS One.* 2010;5(1):e8693.
25. Honsei N, Ikuta T, Kawana K, Kaneko Y, Kawajiri K. Participation of nuclear localization signal 2 in the 3′-ETS domain of FLI1 in nuclear translocation of various chimeric EWS-FLI1 oncoproteins in Ewing tumor. *Int J Oncol.* 2006;29(3):689–693.
26. Miyagawa Y, et al. EWS/ETS regulates the expression of the Dickkopf family in Ewing family tumor cells. *PLoS One.* 2009;4(2):e4634.
27. Surdez D, et al. Targeting the EWSR1-FLI1 oncogene-induced protein kinase PKC-β abolishes Ewing sarcoma growth. *Cancer Res.* 2012;72(17):4494–4503.
28. Richter GH, et al. EZH2 is a mediator of EWS/FLI1 driven tumor growth and metastasis blocking endothelial and neuro-ectodermal differentiation. *Proc Natl Acad Sci U S A.* 2009;106(13):5324–5329.
29. Nishimori H, et al. The Id2 gene is a novel target of transcriptional activation by EWS-ETS fusion proteins in Ewing family tumors. *Oncogene.* 2002;21(54):8302–8309.
30. Smith R, et al. Expression profiling of EWS/FLI1 identifies NKX2.2 as a critical target gene in Ewing's sarcoma. *Cancer Cell.* 2006;9(5):405–416.
31. Kinsey M, Smith R, Lessnick SL. NR0B1 is required for the oncogenic phenotype mediated by EWS/FLI in Ewing's sarcoma. *Mol Cancer Res.* 2006;4(11):851–859.
32. Abaan OD, Levenson A, Khan O, Furth PA, Uren A, Toretsky JA. PTPL1 is a direct transcriptional target of EWS-FLI1 and modulates Ewing's sarcoma tumorigenesis. *Oncogene.* 2005;24(16):2715–2722.
33. Wakahara K, et al. EWS-Fli1 up-regulates expression of the Aurora A and Aurora B kinases. *Mol Cancer Res.* 2008;6(12):1937–1945.
34. Luo W, Gangwal K, Sankar S, Boucher KM, Thomas D, Lessnick SL. GSTM4 is a microsatellite-containing EWS/FLI target involved in Ewing's sarcoma oncogenesis and therapeutic resistance. *Oncogene.* 2009;28(46):4126–4132.
35. Fuchs B, Inwards C, Scully SP, Janknecht R. hTERT is highly expressed in Ewing's sarcoma and activated by EWS-ETS oncoproteins. *Clin Orthop Relat Res.* 2004;426(426):64–68.
36. Watanabe G, et al. Induction of tenascin-C by tumor-specific EWS-ETS fusion genes. *Genes Chromosomes Cancer.* 2003;36(3):224–232.
37. Deneen B, Hamidi H, Denny CT. Functional analysis of the EWS/ETS target gene uridine phosphorylase. *Cancer Res.* 2003;63(14):4268–4274.
38. Hahm KB, et al. Repression of the gene encoding the TGF-beta type II receptor is a major target of the EWS-FLI1 oncoprotein. *Nat Genet.* 1999;23(2):222–227.
39. Dohjima T, Ohno T, Banno Y, Nozawa Y, Wen-yi Y, Shimizu K. Preferential down-regulation of phospholipase C-beta in Ewing's sarcoma cells transfected with antisense EWS-Fli-1. *Br J Cancer.* 2000;82(1):16–19.
40. Scotlandi K, et al. Insulin-like growth factor I receptor-mediated circuit in Ewing's sarcoma/peripheral

neuroectodermal tumor: a possible therapeutic target. *Cancer Res.* 1998;56(20):4570–4574.
41. Balamuth NJ, Womer RB. Ewing's sarcoma. *Lancet Oncol.* 2010;11(2):184–192.
42. Niehrs C. Function and biological roles of the Dickkopf family of Wnt modulators. *Oncogene.* 2006;25(57):7469–7481.
43. Mikheev AM, Mikheeva SA, Liu B, Cohen P, Zarbl H. A functional genomics approach for the identification of putative tumor suppressor genes: Dickkopf-1 as suppressor of HeLa cell transformation. *Carcinogenesis.* 2004;25(1):47–59.
44. Uren A, Wolf V, Sun YF, Azari A, Rubin JS, Toretsky JA. Wnt/Frizzled signaling in Ewing sarcoma. *Pediatr Blood Cancer.* 2004;43(3):243–249.
45. Garnett MJ, et al. Systematic identification of genomic markers of drug sensitivity in cancer cells. *Nature.* 2012;483(7391):570–575.
46. Deneen B, Denny CT. Loss of p16 pathways stabilizes EWS/FLI1 expression and complements EWS/FLI1 mediated transformation. *Oncogene.* 2001;20(46):6731–6741.
47. Sohn EJ, Li H, Reldy K, Beers LF, Christensen BL, Lee SB. EWS/FLI1 oncogene activates caspase 3 transcription and triggers apoptosis in vivo. *Cancer Res.* 2010;70(3):1154–1163.
48. Riggi N, et al. EWS-FLI-1 modulates miRNA145 and SOX2 expression to initiate mesenchymal stem cell reprogramming toward Ewing sarcoma cancer stem cells. *Genes Dev.* 2010;24(9):916–932.
49. Grier HE. The Ewing family of tumors: Ewing's sarcoma and primitive neuroectodermal tumors. *Pediatr Clin North Am.* 1997;44(4):991–1004.
50. Soliman H, Ferrari A, Thomas D. Sarcoma in the young adult population: An international view. *Sem Oncol.* 2009;36(3):227–236.
51. Martins AS, et al. A pivotal role for heat shock protein 90 in Ewing sarcoma resistance to anti-insulin-like growth factor 1 receptor treatment: in vitro and in vivo study. *Cancer Res.* 2008;68(15):6260–6270.
52. Glade Bender JL, et al. Phase I pharmacokinetic and pharmacodynamics study of pazopanib in children with soft tissue sarcoma and other refractory solid tumors: a children's oncology group phase I consortium report. *J Clin Oncol.* 2013;31(24):3034–3043.
53. Jin G, et al. Trib1 and Evi1 cooperate with Hoxa and Meis1 in myeloid leukemogenesis. *Blood.* 2007;109(9):3998–4005.
54. Kawamura-Saito M, et al. Fusion between CIC and DUX4 up-regulates PEA3 family genes in Ewing-like sarcomas with t(4;19)(q35;q13) translocation. *Hum Mol Genet.* 2006;15(13):2125–2137.
55. Pittenger MF, et al. Multilineage potential of adult human mesenchymal stem cells. *Science.* 1999;284(5411):143–147.
56. Sakaguchi Y, Sekiya I, Yagishita K, Muneta T. Comparison of human stem cells derived from various mesenchymal tissues: superiority of synovium as a cell source. *Arthritis Rheum.* 2005;52(8):2521–2529.
57. Shiota M, et al. Isolation and characterization of bone marrow-derived mesenchymal progenitor cells with myogenic and neuronal properties. *Exp Cell Res.* 2007;313(5):1008–1023.
58. Kanno J, et al. "Per cell" normalization method for mRNA measurement by quantitative PCR and microarrays. *BMC Genomics.* 2006;7:64.
59. Fujino T, et al. Function of EWS-POU5F1 in sarcomagenesis and tumor cell maintenance. *Am J Pathol.* 2010;176(4):1973–1982.
60. Subramanian A, Kuehn H, Gould J, Tamayo P, Mesirov JP. GSEA-P: a desktop application for gene set enrichment analysis. *Bioinformatics.* 2007;23(23):3251–3253.
61. Henderson SR, et al. A molecular map of mesenchymal tumors. *Genome Biol.* 2005;6(9):R76.
62. Schaefer KL, et al. Microarray analysis of Ewing's sarcoma family of tumours reveals characteristic gene expression signatures associated with metastasis and resistance to chemotherapy. *Eur J Cancer.* 2008;44(5):699–709.
63. Nakayama R, et al. Gene expression analysis of soft tissue sarcomas: characterization and reclassification of malignant fibrous histiocytoma. *Mod Pathol.* 2007;20(7):749–759.
64. Albino D, et al. Identification of low intratumoral gene expression heterogeneity in neuroblastic tumors by genome-wide expression analysis and game theory. *Cancer.* 2008;113(6):1412–1422.
65. Barretina J, et al. Subtype-specific genomic alterations define new targets for soft-tissue sarcoma therapy. *Nat Genet.* 2010;42(8):715–721.
66. Haldar M, et al. A conditional mouse model of synovial sarcoma: insights into a myogenic origin. *Cancer Cell.* 2007;11(4):375–388.
67. Teitz T, et al. Th-MYCN mice with caspase-8 deficiency develop advanced neuroblastoma with bone marrow metastasis. *Cancer Res.* 2013;73(13):4086–4097.
68. Jeannet R, et al. Oncogenic activation of the Notch1 gene by deletion of its promoter in Ikaros-deficient T-ALL. *Blood.* 2010;115(25):5443–5454.
69. Nakayama R, et al. Gene expression profiling of synovial sarcoma: distinct signature of poorly differentiated type. *Am J Surg Pathol.* 2010;34(11):1599–1607.
70. Masque-Soler N, Szczepanowski M, Kohler CW, Spang R, Klapper W. Molecular classification of mature aggressive B-cell lymphoma using digital multiplexed gene expression on formalin-fixed paraffin-embedded biopsy specimens. *Blood.* 2013;122(11):1985–1986.
71. Tanaka M, Jin G, Yamazaki Y, Takahara T, Takuwa M, Nakamura T. Identification of candidate cooperative genes of the Apc mutation in transformation of the colon epithelial cell by retroviral insertional mutagenesis. *Cancer Sci.* 2008;99(5):979–985.

Integrative knowledge management to enhance pharmaceutical R&D

Maria Marti-Solano, Ewan Birney, Antoine Bril, Oscar Della Pasqua, Hiroaki Kitano, Barend Mons, Ioannis Xenarios and Ferran Sanz

Information technologies already have a key role in pharmaceutical research and development (R&D), but achieving substantial advances in their use and effectiveness will depend on overcoming current challenges in sharing, integrating and jointly analysing the range of data generated at different stages of the R&D process.

Maria Marti-Solano and Ferran Sanz are at the IMIM and Universitat Pompeu Fabra, Dr. Aiguader 88, 08003 Barcelona, Spain.
Ewan Birney is at the European Molecular Biology Laboratory, European Bioinformatics Institute, Hinxton, Cambridgeshire CB10 1SD, UK.
Antoine Bril is at the Institut de Recherches Internationales Servier, 53 rue Carnot, 92284 Suresnes Cedex, France.
Oscar Della Pasqua is at GlaxoSmithKline, Stockley Park West, Uxbridge, Middlesex UB11 1BT, UK.
Hiroaki Kitano is at the Systems Biology Institute, 5-6-9 Shirokanedai, Minato, Tokyo 108–0071, Japan; and the RIKEN Center for Integrative Medical Sciences, 1-7-22 Suehiro-cho, Tsurumi-ku, Yokohama City, Kanagawa 230–0045, Japan.
Barend Mons is at the Netherlands Bioinformatics Centre, 260 NBIC, 6500 HB Nijmegen, The Netherlands; and the Leiden University Medical Center, Albinusdreef 2, 2333 ZA Leiden, The Netherlands.
Ioannis Xenarios is at the Swiss Institute of Bioinformatics, Quartier Sorge - Batiment Genopode, 1015 Lausanne, Switzerland.
Correspondence to F.S.
e-mail: ferran.sanz@upf.edu
doi:10.1038/nrd4290

The explosion in the accumulation of biomedical data resulting from technological advances such as next-generation sequencing, coupled with progress in information technologies, offers new opportunities to use such information for pharmaceutical R&D. In parallel, the increasingly collaborative nature of many R&D projects has highlighted the importance of effective information sharing between project partners and, from a wider perspective, with the overall biomedical community.

Initiatives such as the European Innovative Medicines Initiative (IMI) are supporting the development of strategies aimed at improving translational knowledge management in biomedical sciences, as well as overcoming barriers in information sharing. In this article, we highlight the key points emerging from a debate on 'Translational Knowledge Management in Pharmaceutical R&D', held in Brussels in July 2013, that involved representatives from a range of collaborative projects in the field, along with other experts and stakeholders (see Supplementary information S1 (box) for details). Challenges that were discussed include the complexity and heterogeneity of biomedical data, the need to establish relevant, widely accepted and openly available data standards and the lack of integration of knowledge from different disciplines and stages of the R&D process.

Key issues and challenges

Data evaluation and integration. Given the complexity of most biological questions, combining data from multiple levels (molecular, cellular, tissue and others), disciplines (molecular and systems biology, medicinal chemistry, preclinical and clinical pharmacology, and others) and sources may be needed to develop information resources and computational models that are useful for addressing pharmaceutical R&D questions effectively. Indeed, the issue of managing data arising from different sources is becoming increasingly important as changes in the R&D ecosystem mean that information is not necessarily generated in-house by large pharmaceutical companies but is derived from external organizations such as academic institutions, biotechnology companies or contract research organizations.

The heterogeneity of biomedical data is a major challenge. In many cases, a key determinant of data usefulness and reusability is the availability of additional information to evaluate the relevance and quality of a particular data set. Being able to track the data source and to retrieve information on the context in which the data were generated (for example, experimental conditions and the model organisms used) is crucial to assess whether the data are suitable to address a particular research question and, moreover, whether data from different sources can be meaningfully combined. In addition, to perform large-scale statistical analyses and generate useful models from biomedical data, it is necessary to have not only information on the positive results but also on the negative or discarded ones.

Ontologies and standards. Developing, disseminating and promoting the wide-scale adoption of appropriate biomedical ontologies and data standards is also crucial in allowing data integration. The definition and usage of standards for the characterization of experimental assays, for the collection of clinical information, for model description and, in general, for the representation of different types of metadata, will facilitate true data interoperability — that is, a meaningful and accurate exchange, integration and joint exploitation of biomedical data[1]. In order to promote the broad adoption of such standards, it is important that they are open and reasonably flexible, and that key stakeholders and user communities are engaged with their development. In some areas, these aims may be best served by a bottom-up approach, whereas others will require a coordinated top-down initiative.

An example of a high-impact top-down initiative is the recent commitment by the European Medicines Agency (EMA), the Japanese Pharmaceutical & Medical Devices Agency (PMDA) and the US Food and Drug Administration (FDA) to require data standards developed by the Clinical Data Interchange Standards Consortium (CDISC).

Data and information sharing. Another of the major challenges for the effective integration of data relevant to pharmaceutical R&D is that data, associated information and knowledge often remain siloed[2]. Moreover, there are communication barriers between researchers from different disciplines. So, not only the data but also relevant details about it need to be shared. This requires assessment of the relevance of data, taking into account the underlying clinical or biomedical research question and adapting the information to suit its use across different areas of expertise. This could be achieved by identifying the crucial information and tailoring the key messages that are required for decision-making at different stages of drug discovery and development, while promoting the traceability of data. This is helped by training and involving specific professionals (knowledge engineers and data scientists) who are capable of bridging information silos and facilitating communication and collaboration[3].

Active involvement of the community is the basis for successful integrative knowledge management in R&D. This may require the creation of regulations to generate confidence about data sharing and the promotion of information formats that facilitate it. It is possible to harness the know-how of the research community by throwing down scientific challenges, involving the community in knowledge extraction, annotation and filtering[4]. Furthermore, the availability of novel communication channels (such as social networks) and the increasing availability of individual genetic information owing to the decrease in sequencing costs will affect current research models and could make patient participation in the R&D process more active.

Data sustainability. Ensuring sustainability of data repositories in the long term — including their maintenance as well as their updating and evolution in a changing environment — should be a key component of collaborative projects. Making data accessible to a wider community and enabling their reuse beyond the project that generates them will be crucial to optimize the use of resources by minimizing replication. We therefore believe that data sharing should become a requirement when public funding is involved. However, to empower the scientific community to effectively reuse data, it has to be enriched with relevant metadata, and published data should be converted into appropriate formats for integrative knowledge management[5]. Similarly, computational models that are developed to enable data representation must be maintained and updated, as well as systematically characterized by appropriate metadata that allow further appraisal of their predictive performance and possible biases.

Recommendations

To maximize the effectiveness of efforts to integrate data in pharmaceutical R&D, it is vital to develop strategies and processes to ensure that:

- Protocol design and data collection focus on questions that are relevant for decision-making at the different stages of pharmaceutical R&D
- Relevant standards for the characterization of data, methods and models are identified (or developed if unavailable) and their use is promoted and facilitated by dissemination and training
- Data and models are annotated with enough detail regarding their provenance and quality to allow a critical assessment of their suitability for reuse
- Data sharing is understood as a responsibility (especially when data are derived from public funding), and the community participates in the promotion and recognition of data sharing, as well as in knowledge extraction and management
- Sustainability of data collections is considered a key component in the life cycle of collaborative projects

The dissemination and adoption of these principles among stakeholders — and in particular across the scientific community, clinical researchers and policy makers — is essential to establish knowledge management strategies in pharmaceutical R&D that efficiently exploit the increasing availability of novel biomedical data and learn from previous experience, thus enabling a more efficient search for innovative, effective and safe medicines.

1. Sansone, S. A. *et al.* Toward interoperable bioscience data. *Nature Genet.* **44**, 121–126 (2012).
2. Cases, M. *et al.* Improving data and knowledge management to better integrate health care and research. *J. Intern. Med.* **274**, 321–328 (2013).
3. Beck, T. *et al.* Knowledge engineering for health: a new discipline required to bridge the "ICT gap" between research and healthcare. *Hum. Mutat.* **33**, 797–802 (2012).
4. Kitano, H. *et al.* Social engineering for virtual 'big science' in systems biology. *Nature Chem. Biol.* **7**, 323–326 (2011).
5. Williams, A. J. *et al.* Open PHACTS: semantic interoperability for drug discovery. *Drug Discov. Today* **17**, 1188–1198 (2012).

Acknowledgements

The debate on "Translational Knowledge Management in Pharmaceutical R&D" was held in Brussels on 11–12 July 2013, within the framework of the European INBIOMEDvision CSA (funded by the EU FP7 under grant agreement no. 270107) and with the collaboration of Innovative Medicines Initiative (IMI). In addition to the authors, A. Martin, R. Bellazzi, N. Blomberg, A. Brookes, R. Campbell, B. de Bono, I. Dix, G. Ecker, Y. Guo, B. Hardy, M. Hofmann-Apitius, J. Houwing-Duistermaat, L. D. Hudson, B. Kisler, J. Kleinjans, V. Maojo, J. Mestres, J.L. Oliveira, M. Pastor, T. Rijnders, S. Scollen, T. Steger-Hartmann, P. Ruch, T. Slater, G. O. Strawn, M. Sundgren, J. van der Lei and M. Goldman were speakers at the debates and are acknowledged for their valuable input and support for the ideas in this paper, which represent the consensus view of all the participants (see Supplementary information S1 (box) for their affiliations).

Competing interests

The authors declare no competing interests.

SUPPLEMENTARY INFORMATION

See online article: S1 (box)

ALL LINKS ARE ACTIVE IN THE ONLINE PDF